Contract No. Nonr 839(58)

IMPURITY PHOTOIONIZATION THEORY OF PRECURSORS

by

Daniel S. Wilson and Tony C. Lin

OCTOBER 1967

POLYTECHNIC INSTITUTE OF BROOKLYN

DEPARTMENT
of
AEROSPACE ENGINEERING
and
APPLIED MECHANICS

PIBAL REPORT NO. 1006

IMPURITY PHOTOIONIZATION THEORY OF PRECURSORS

by

Daniel S. Wilson and Tony C. Lin

The research has been conducted under Contract Nonr 839(38) for PROJECT DEFENDER, and was made possible by the support of the Advanced Research Projects Agency under Order No. 529 through the Office of Naval Research.

Polytechnic Institute of Brooklyn

Department

of

Aerospace Engineering and Applied Mechanics

October 1967

PIBAL REPORT NO. 1006

IMPURITY PHOTOIONIZATION THEORY OF PRECURSORS[†]

by

Daniel S. Wilson[*] and Tony C. Lin[**]

Polytechnic Institute of Brooklyn, Graduate Center
Farmingdale, New York

ABSTRACT

An extension of Wetzel's theory is proposed to explain electron precursor phenomena in pressure driven shock tubes. The theory is based on the assumption, which has been experimentally verified, that radiation from the hot gas behind the shock front is responsible for the precursor effect. A point radiator, located at the shock front and moving with the shock velocity, is assumed. It is shown that this radiator can be idealized by a black body. The precursor electron density is derived from a one-step photoionization of the impurities present in the driven gas.

As an application of the theory, precursor profiles are calculated for an H_2 impurity. The partial pressure of H_2 is varied from 2 to 75μ Hg. The temperature behind the shock is assumed to be 11,000°K.

[†] This research was supported under Contract Nonr 839(38) for PROJECT DEFENDER, and the Advanced Research Projects Agency under Order No. 529 through the Office of Naval Research.

[*] Assistant Professor of Aerospace Engineering

[**] Research Fellow

TABLE OF CONTENTS

LIST OF ILLUSTRATIONS

SECTION I

INTRODUCTION

Upon reentry of a satellite or meteor into the earth's atmosphere, many investigators observed ionization far in front of the shock wave of the reentering body. S. C. Lin[1] and his co-workers, through their radar measurements, established that high electron densities are found several meters ahead of the shock of a manned satellite. Cook and Hawkins[2] also found detectable electron densities in front of reentering meteors. Prior to these observations, a number of investigators working with shock tubes observed signals on probes far in front of the shock. All these signals became known as precursor phenomena.

The precursor ionization is important for a number of reasons. First, the problem of discrimination of reentering bodies may be highly affected because this phenomena may change measurably the radar cross-section of reentering bodies. Secondly, since the precursor ionization must be associated with energy transfer from behind the shock to in front of the shock, the conventionally assumed shock structure may have to be modified to take into account this energy transfer. Thirdly, precursor ionization causes the shock front to pass through a partially ionized gas, and this may affect the chemical reactions taking place behind the shock.

Several hypotheses have been advanced to explain precursor phenomena. According to one hypothesis, the shock heated gas radiates U. V. and X-rays which photoionizes the gas in front of the shock[3]. This ionization may be a one-step process from the ground state of the gas, or it may be a two-step process where the atom is first excited and then ionized. Also the source, the shock heated gas, may behave as a continuum

black body radiator or line radiation may be significant. Recently, Clarke[4] and Murty[5] have suggested that line radiation plays a significant role in precursor phenomena.

Another hypothesis begins with the recognition that a large electron and ion density gradient exists at the shock front. This would result in a strong tendency for the electrons and ions to diffuse into the precursor region. Weyman[6] claimed experimental verification for electrons escaping from behind the shock with velocities several times larger than the shock velocity. A critical theoretical study of this diffusion hypothesis by Petschek[7] and Wetzel[3] concluded that this phenomena can be completely neglected in the precursor region except in a region about one Debye length ahead of shock front. The theoretical models mentioned above do not involve the gas dynamics of the shock in any essential way; i. e., the basic equations of fluid mechanics are uncoupled from the equations of radiation transport.

Besides these two hypotheses, there are some other postulations suggested to explain this ionization phenomena. Hollyer[8] and Gloersen[9] attribute the precursor to the effect of photoemission from the walls of shock tube. Photoemission would leave an insulated shock tube wall positively charged and only electrons would be collected by electrostatic probes. However, the presence of large numbers of positive ions have been found in the precursor region[10].

Lederman and Wilson[10] applied a microwave resonant cavity technique to measure precursor profiles. This technique avoids the difficulties and uncertainties of interpreting probe signals. The cavity technique yields definite values of electron density while the probe measurements give only the shape of the precursor profile and not always the absolute

electron number density. Lederman and Wilson's experiments concluded that: (1) the precursor ionization is due to radiation from the shocked gas behind the incident shock; (2) the electron precursor velocity is equal to the shock velocity.

Hammerling[11] and S. C. Lin[1] analyzed the precursor phenomena for a satellite reentering the atmosphere by assuming that the ultraviolet radiation comes from the $b'^1\Sigma_u^+ \rightarrow X^1\Sigma_g^+$ transition of N_2. This radiation then precedes the shock into the unshocked gas and ionizes the molecular oxygen. They found that the precursor ionization halo appears satisfactory for explaining the leading edge echo before the MA-6 Mercury capsule. It is worthy to note that their model is based on a one step ionization process.

So far, the important role that impurities may play in precursor ionization has not been emphasized in the literature. This is true even though Petschek[7] and Sturtevant[12] recognized that impurities play a dominating role in initiating ionization in high temperature gases behind shocks.

In this paper a one-step photoionization theory will be presented. This theory is based on a Wetzel-type[3] model with several important modifications. The important role that impurities play in precursor ionization will be emphasized.

The authors would like to thank Prof. Samuel Lederman for many enlightening discussions during the course of this work.

SECTION II

PHOTOIONIZATION THEORY OF PRECURSOR IONIZATION

The mechanism proposed by Wetzel views the shock wave as a radiator moving at the shock speed; this radiator ionizes the gas ahead of the shock, producing the precursor. The experiments of Ref. 10 suggest this type of mechanism.

II. A. Review of Wetzel's Theory

A one-dimensional, shock-based coordinate system is assumed in Fig. 1. In this coordinate system the gas is streaming in the minus x-direction at the shock velocity, U. Steady state conditions are assumed. The governing equations, momentum transport equations for electrons and for ions and Poisson's equation to provide electrostatic coupling between the two charged species, follow:

$$D_e \frac{d^2 n_e}{dx^2} + \mu_e \frac{d}{dx}(E n_e) + U \frac{dn_e}{dx} = -r(x) + s(x) \tag{1}$$

$$D_i \frac{d^2 n_i}{dx^2} - \mu_i \frac{d}{dx}(E n_i) + U \frac{dn_i}{dx} = -r(x) + s(x) \tag{2}$$

$$\varepsilon_o \frac{dE}{dx} = e(n_i - n_e) \tag{3}$$

where n_e and n_i are the electron and ion densities, and D_e, μ_e and D_i, μ_i are the respective diffusion and mobility coefficients of electrons and ions relative to the flow velocity, U. E is the electrostatic field, and r(x) and s(x) are source and sink functions, respectively. Eq. (1), for example, is simply a balance equation for electrons. The first term on the left is a net loss due to diffusion, the second term a loss due to electric forces, and the third is the familiar conduction term; this is balanced on the right by sink and source terms.

The sink term, $s(x)$, is due to losses such as recombination. Such losses are unimportant in the present application, and $s(x)$ will therefore be dropped from the equations. The source term, $r(x)$, introduces additional electrons and ions due to photoionization, and it is this term which has to be further investigated.

We define a partial source function, $r(x;\nu)\, d\nu$, as the number of ionizations per unit volume per second produced at x by photons in the frequency range from ν to $\nu + d\nu$. With each $r(x;\nu)\, d\nu$ we will associate a partial ionization density, $n(x;\nu)d\nu$, with each range of photon frequencies. The total source and density functions then become

$$r(x) = \int_{\nu_i}^{\infty} r(x;\nu)d\nu$$

$$n(x) = \int_{\nu_i}^{\infty} n(x;\nu)d\nu \qquad (4)$$

where ν_i is the lowest ionization frequency of the gas in the precursor region.

Now let $N(\nu)$ be the number of photons emitted per unit area per second per unit frequency range by the radiator located at $x = 0$. The probability that a photon of frequency ν will penetrate a distance x and be absorbed between x and $x + dx$ is then

$$n_g\, Q(\nu) \exp\left[- n_g\, Q(\nu)\, x\right] dx \qquad (5)$$

where n_g is the number density of the gas particles in the precursor region and $Q(\nu)$ is the absorption cross-section of photons of frequency ν in the gas. If $Q_i(\nu)$ is the ionization cross-section for photons of frequency ν, then $Q_i(\nu)/Q(\nu)$ is the probability that an absorbed photon will produce an ionization, and $r(x;\nu)$ is given by

$$r(x;\nu) = N(\nu)\, n_g\, Q_i(\nu) \exp\left[-\, n_g Q(\nu)\, x\right] \tag{6}$$

From the experimental results in Ref. 10, we can neglect all terms involving diffusion, since the precursor profile is caused by photoionization only. Thus, the first two terms in Eqs. (1) and (2) will be dropped, leaving simply

$$-\, U \frac{dn(x;\nu)}{dx} = N(\nu)\, n_g\, Q_i(\nu) \exp\left[-\, n_g\, Q(\nu)\, x\right] = r(x;\nu) \tag{7}$$

where a distinction betwen electron and ion distribution is no longer necessary. Now, we will assume that the shock is moving at nearly constant velocity. This implies that the attenuation of shock strength is negligible. This assumption is also verified experimentally.

We can integrate Eq. (7) with respect to x from ∞ to x using the boundary condition that $n(\infty;\nu) = 0$; and also integrating with respect to ν, we find the total ionization density:

$$n(x) = U^{-1} \int_{\nu_i}^{\infty} N(\nu)\, \frac{Q_i(\nu)}{Q(\nu)} \exp\left[-\, n_g\, Q(\nu)\, x\right] d\nu \tag{8}$$

To further simplify Eq. (8), let us define $f(\nu) = Q(\nu)/Q(\nu_i)$ as the absorption cross-section normalized to its value at the ionization edge, and $\eta = \frac{x}{\lambda_i}$ as a dimensionless distance upstream of the radiator (where $\lambda_i = 1/n_g\, Q(\nu_i)$ is the photon mean free path at the ionization edge). In terms of $f(\nu)$ and η, Eq. (8) can be written

$$n(\eta) = U^{-1} \int_{\nu_i}^{\infty} N(\nu)\, f(\nu)^{-1} \exp\left[-\, f(\nu)\eta\right] d\nu \tag{9}$$

II. B. Precursor Distribution in Argon

It is first assumed that the shock front radiates as a black body at a temperature equal to the temperature behind the shock, and that it is the high energy photons of this radiation that are responsible for the precursor. Using the high energy limit of the black body curve, we get

$$N(\nu) = \frac{2\pi}{c^2} \nu^2 \exp\left[-\frac{h\nu}{KT}\right], \quad h\nu >> KT \tag{10}$$

For many absorption processes, it can be assumed that each absorbed photon produces an ion pair. For such processes we have $Q_i(\nu)/Q(\nu) = 1$. This is approximately correct for inert gases, such as Argon. From 790Å (which corresponds to the first ionization potential of Argon) to about 420Å, the cross-section, $Q(\nu)$, for Argon is fairly constant and equal to about 35×10^{-18} cm^2. For wave lengths smaller than 420Å, the cross-section falls off approximately as ν^{-3}. Therefore, in the calculation, the following values of $f(\nu)$ are used:

$$\begin{aligned} f(\nu) &= 1 && \text{for } 420\text{Å} < \lambda < 790\text{Å} \\ f(\nu) &= \left[\frac{\nu_{420\text{Å}}}{\nu}\right]^3 && \text{for } \lambda < 420\text{Å} \end{aligned} \tag{11}$$

Using Eqs. (10) and (11) in Eq. (9), one can find $n(\eta)$ as a function of η. The calculated distribution falls off much too rapidly to explain the observed precursor [10, 13]. For example, at 50 cm. ahead of shock, the calculated number density is 5 orders of magnitude below the observed value [10, 12].

The electron number density at the shock front is obtained by letting $\eta \to 0$ in Eq. (9):

$$n(0) = U^{-1} \int_{\nu_i}^{\infty} \frac{N(\nu)d\nu}{f(\nu)} \qquad (12)$$

This is simply an integral over the tail of the black body distribution and can readily be calculated. The value n(0) is approximately 10^{14} el. /c. c. as compared to 10^{16} el. /c. c. in the equilibrium region behind the shock front.

Wetzel's model failed to fit the experimental results [10, 13]. However, both theory[4, 3, 9] and experiment[10,13] strongly suggest that "radiation" plays the dominant role in precursor ionization phenomena. Thus, it is necessary to modify Wetzel's theory or develop a new theory, one which is intimately tied to the "radiation" hypothesis, to explain this phenomena.

SECTION III

MODIFICATIONS IN THE PHOTOIONIZATION THEORY

Wetzel, as described in Section IIA, assumes a plane source, infinite in extent, in deriving his relations for the precursor profile ahead of the shock. We do not feel this is a realistic assumption to make for any practical confirmation of his theory, the source is seldom of this type. For example, for a reentering vehicle, the source behaves as a point radiator located at the nose of the vehicle, and some account must be taken of the fact that the radiation falls off as the inverse square of the distance from the vehicle even if there is no absorption of the radiation. Also, in the shock tube, the diameter of the shock tube is small compared to the distance ahead of the shock where measurements are of interest, and it is more realistic to assume a point source at the shock front than a plane radiator.

In this paper a point radiator, located at the shock front, is assumed. At the frequencies of interest, it can safely be assumed that all radiation impinging on walls of the shock tube is completely absorbed. Since the radiation will now "fall off" faster than for a one-dimensional radiator, a one-step photoionization of Argon will still not supply the answer to what is responsible for the precursor. In this paper, the important role that impurities in the driven gas of the shock tube have on the nature of the precursor will be emphasized.

III.A. The Electron Precursor Distribution

If a point source is assumed, Eq. (6) becomes

$$r(x;\nu) = \frac{A}{4\pi x^2} N(\nu)\, n_g\, Q_i(\nu) \exp\left[-\, n_g\, Q(\nu)\, x\right] \qquad (13)$$

where A is the cross-sectional area of the shock tube. It is assumed

that our measurements are made far enough from the source that the radiation flux is everywhere in the axial direction.

This is inserted into Eq. (7), and the integration is again from ∞ to x:

$$n(x;\nu) = - \frac{A}{4\pi U} \; n_g \, N(\nu) \, Q_i(\nu) \int_{\infty}^{x} \frac{1}{x^2} \exp\left[- n_g \, Q(\nu) x \right] dx \qquad (14)$$

Integrating Eq. (14) by parts, we get

$$n(x;\nu) = - \frac{A}{4\pi U} \; n_g \, N(\nu) \, Q_i(\nu) \left\{ - \frac{1}{x} \exp \left[- n_g \, Q(\nu) \, x \right] \right. \qquad (15)$$

$$\left. - n_g \, Q(\nu) \int_{\infty}^{x} \frac{1}{x} \exp\left[- n_g \, Q(\nu) \, x \right] dx \right\}$$

The integral on the right side of Eq. (15) can be written as follows

$$\int_{\infty}^{x} \frac{1}{x} \exp \left[- n_g \, Q(\nu) \, x \; dx \right] = \int_{-\infty}^{-n_g \, Q(\nu) x} \frac{e^t}{t} \, dt \qquad (16)$$

$$= Ei \left[- n_g \, Q(\nu) \right] x = Ei(- \xi)$$

where $\xi = n_g \, Q(\nu) \, x$.

The function $Ei(-\xi)$ is the well-known exponential integral [14, 15]; its series expansions can be written as:

$$Ei(-\xi) = \gamma + \ell n \, \xi + \sum_{n=1}^{\infty} \frac{(-1)^n \xi^n}{n(n!)} \; , \quad (\xi > 0) \qquad (17)$$

where

$$\gamma = \lim_{n \to 0} \left[1 + \frac{1}{2} + \frac{1}{3} + \ldots + \frac{1}{n} - \log n \right] = 0.577$$

(γ is called Euler or Mascheroni's constant)

For $\xi >> 1$, $Ei(-\xi)$ has the following asymptotic representation:

$$Ei(-\xi) = \frac{e^{-\xi}}{(-\xi)} \left[1 - \frac{1!}{\xi} + \frac{2!}{\xi^2} - \frac{3!}{\xi^3} + \ldots .\right] \tag{18}$$

In terms of $Ei(-\xi)$, Eq. (15) can be written

$$n(x;\nu) = -\frac{A}{4\pi U} n_g N(\nu) Q_i(\nu) \left\{ -\frac{1}{x} \exp\left[-n_g Q(\nu) x\right] - n_g Q(\nu) Ei(-\xi) \right\} \tag{19}$$

The total number density, $n(x)$, is obtained by integrating Eq. (19) with respect to ν,

$$n(x) = \frac{A n_g}{4\pi U} \left\{ \int_{\nu_i}^{\infty} \frac{N(\nu) Q_i(\nu)}{x} \exp\left[-n_g Q(\nu) x\right] d\nu + n_g \int_{\nu_i}^{\infty} N(\nu) Q_i(\nu) Q(\nu) Ei(-\xi) d\nu \right\} \tag{20}$$

Equation (20) now becomes the revised form of Eq. (9) in the new theory. It should be mentioned again that Eq. (20) will cause an even faster decrease with distance in the precursor electron concentration than given by the theory of Section IIA, since the source radiation falls off faster. For this reason, the conclusions reached in Section IIB concerning an Argon photoionization interpretation of the precursor phenomenon will not change.

III. B. The Black Body Assumption

The radiant energy required for photoionization of the gases ahead of shock waves comes from the shock heated high-temperature gas behind the shock front. Thus, it is necessary to know the time history of the light

intensity, the spectrum, and the absorption coefficients of radiating sources before an accurate prediction of the precursor profile is possible. It is difficult to analyze this non-steady, non-equilibrium radiating source behind the shock analytically and, unfortunately, spectrum data for shock heated gases are also virtually non-existent.

Petschek and Byron[7] and Blackman and Niblett[16] studied relaxation processes behind Argon shocks and found, experimentally, that the relaxation time was strongly dependent on the impurity content of the Argon driven gas. Recently, Sturtevant[12] applied a mass spectrometer to study the ionization processes and chemical species behind an Argon shock. He found a large amount of O^+ and H^+ (about five times more abundant than Argon) during the initial stages of ionization. The small amount of impurities, he concluded, played a dominant role in the ionization process, or at least in the initial ionization.

In Section IIA the precursor ionization profile is calculated by assuming that the shock is a black body radiator, i.e., the radiating source is optically thick. This is a reasonable assumption to make for frequencies above the first ionization edge of Argon. However, for frequencies below this ionization edge, the radiation is not necessarily expected to behave like black body radiation. Due to impurities in the driven gas, it may still be safe to make a black body assumption. An attempt will be made in the present section to answer this question.

The equation for radiative transfer in steady case at the absence of scattering is

$$\frac{\partial I_\nu}{Z} = (\rho j_\nu - k_\nu I_\nu) \qquad (21)$$

where

ρj_ν = emission coefficient

k_ν = absorption coefficient

I_ν = intensity of radiation

Under the assumption of thermodynamic equilibrium in the shocked heated gas, Eq. (21) reduces to

$$\frac{\partial I_\nu}{\partial Z} = k_\nu (B_\nu - I_\nu) \tag{22}$$

where

$$B_\nu(\nu) = \frac{2h\nu^3/c^2}{e^{h\nu/kT} - 1} \tag{23}$$

After integrating Eq. (22) and using the boundary condition that $I_\nu = 0$ at $Z = 0$ (at the contact surface), we get

$$I_\nu = B_\nu \left[1 - e^{-k_\nu Z}\right] \tag{24}$$

The total radiation intensity is

$$I = \int_o^\infty B_\nu(\nu) (1 - e^{-k_\nu Z}) \, d\nu \tag{25}$$

The unknown in Eq. (25) is the absorption coefficient "k_ν" which is a function of temperature as well as frequency. If $k_\nu Z >> 1$, it is optically thick and I_ν will be very similar to a black body emitter.

There are a variety of mechanisms for emission and absorption of radiation which are associated with transitions between energy levels of the gas atoms or molecules. In these transitions, the change in internal energy of the atom is equal to the radiant energy absorbed. The types of transitions that are important in a given situation depends on the

nature of the gas, on the distribution of molecules among the various energy levels, and on the radiant frequency range of interest. They can be roughly classified as 3 kinds, i. e.; bound-bound, bound-free, and free-free transitions. Bound-bound transition gives rise to a discrete line spectrum (the contribution of this type of transition will be neglected in this report), while free-free and bound-free transitions give rise to a continuous spectrum.

The composite gas molecules in the high temperature region consists mainly of Argon with some impurities or trace gases such as dissociated air molecules (oxygen or nitrogen), etc. However, the exact amount of impurities mixing with the Argon is not known.

Under quasi-equilibrium conditions, the absorption coefficient k_ν can be estimated by the existing theories. The first step is to evaluate the population of various atomic and molecular energy levels. This includes the calculation of dissociation and the degree of ionization. The second, a problem in quantum theory of radiation, is the calculation of the radiative transition probability for transition between the different energy levels. This problem is very difficult, and experimental data will be used.

The primary impurity in the driven gas is assumed to be O_2 (15μ Hg). For an initial pressure of P_1 = 2 mm Hg Argon and a Mach number of 13.2, the temperature behind the incident shock is approximately 11,000°K. The O_2 density jump across the shock is assumed to be the same as for the Argon, and the O_2 behind the incident shock is assumed to be fully dissociated. The table gives the calculated values for k_ν for atomic oxygen[17] for wave lengths between 930$\mathring{A}$ and 600$\mathring{A}$.

Table: Absorption Coefficients of Atomic Oxygen

P_1 (argon) = 2 mm Hg.

M = 13.2

Initial O_2 Pressure = 15μHg.

λ(Å)	930	900	870	830	800	770	730	700	600
k_ν (cm^{-1})	4.1×10^{-2}	4.1×10^{-2}	4.2×10^{-2}	4.6×10^{-2}	4.9×10^{-2}	8.6×10^{-1}	1.1×10^{-1}	1.1×10^{-1}	1.1×10^{-1}

A typical value of k_ν for atomic oxygen is 4×10^{-2} cm^{-1}. For a radiating source of 10 cm in length (distance between shock front and contact surface), $k_\nu x = .4$.

Thus, from Eq. (24), we get:

$$I_\nu = B_\nu (1 - e^{0.4}) = 0.35 B_\nu$$

Thus, the photon emitter is about 35% efficient and can be idealized as a black body emitter.

III. C. Variation in the Precursor Profile with Impurity Partial Pressure

The theory predicts that a plot of precursor electron number density versus impurity partial pressure, for fixed distance ahead of shock, should peak at a certain value of impurity partial pressure. This can be seen from the following analysis:

If a maximum value of n(x) occurs at a certain impurity partial pressure, p, then

$$\frac{\partial n(x)}{\partial p} = 0, \quad p = p_I \tag{26a}$$

and

$$\frac{\partial^2 n(x)}{\partial p^2} < 0, \quad p = p_I \tag{26b}$$

where p_I = the partial pressure of impurity which will give the ionization profile a peak value.

We differentiate Eq. (20) with respect to p, and recognize that $Q(\nu)$, $Q_i(\nu)$, ν and x are independent of p, while n_g is not. The relationship between p and n_g is

$$p = n_g KT. \tag{27}$$

When we set the derivative equal to zero, we have

$$\frac{\partial n(x)}{\partial p} = \frac{\partial n(x)}{\partial n_g} \frac{\partial n_g}{\partial p} = \frac{1}{KT} \frac{\partial n(x)}{\partial n_g} = 0 \tag{28}$$

for $KT \neq 0$, so $\frac{\partial n(x)}{\partial n_g} = 0$ (29)

Performing the differentiation in Eq. (20) with respect to n_g, we get

$$\frac{\partial n(x)}{\partial n_g} = \int_{\nu_i}^{\infty} n_g \left[N(\nu) Q(\nu) Q_i(\nu) \right] \left\{ \frac{e^{-\xi}}{\xi} + 2 \, Ei(-\xi) \right\} d\nu = 0 \tag{30}$$

where $\xi = n_g Q(\nu) x$.

The second derivation of n(x) with respect to "p" follows:

$$\frac{\partial^2 n(x)}{\partial p^2} = \left[\frac{1}{KT}\right]^2 \int_{\nu_i}^{\infty} [N(\nu)Q(\nu)Q_i(\nu)] [e^{-\xi} + 2Ei(-\xi)] d\nu \qquad (31)$$

We are going to show that $\frac{\partial^2 n(x)}{\partial p^2} < 0$ for certain values of n_g or p.

The exponential integral, Ei(-ξ), is negative in value, i.e., Ei(-ξ) <0; also $N(\nu)Q(\nu)Q_i(\nu) > 0$, $n_g > 0$ and $(kT)^2 > 0$.

Suppose we impose $0 < \xi < 1$ with the range of frequency $\nu_i \leq \nu \leq \infty$; if $\partial n(x)/\partial n_g = 0$ is true, then comparison of Eqs. (30) and (31) leads to the result that $\partial^2 n(x)/\partial p^2 < 0$. This means at least one relative maximum value for n(x) occurs somewhat within $0 < \xi < 1$. On the other hand, if $\xi > 1$ and $\partial n(x)/\partial n_g = 0$ are true, then we can see $\partial^2 n(x)/\partial p^2 > 0$ from Eqs. (30) and (31), so that at least a relative minimum value of n(x) occurs somewhere at $\xi > 1$. In what follows, it will be seen that ξ is usually restricted to values between 0 and 1 and, therefore, we would expect to find maximum values for n(x).

SECTION IV

PHOTOIONIZATION OF A MOLECULAR HYDROGEN IMPURITY

IV. A. "Peak Behavior" for a Molecular Hydrogen Impurity

To evaluate the value of p or n_g that will give the precursor profile a peak value (or $\partial n(x)/\partial n_g = 0$), we have to solve the integral Eq. (30). This equation can be solved by an asymptotic expansion.

A black body emitter, i.e., Eq. (10) will be used and the impurity will now be assumed to be Molecular Hydrogen, whose absorption cross-section can be expressed in closed form as follows:

$$\frac{Q(\nu)}{Q(\nu_i)} = \frac{\nu_i}{\nu}^{*} \tag{32}$$

where $h\nu_i = 15.422$ ev.

Then Eq. (30) can be written as

$$\frac{\partial n(x)}{\partial n_g} = \frac{2\pi}{c^2} Q(\nu_i) \int_{\nu_i}^{\infty} \left\{ f(\nu) \frac{\nu \nu_i}{x} \exp\left[-\frac{h\nu_i}{KT} \left(\frac{\nu}{\nu_i} + \frac{x}{\lambda_i} \frac{\nu_i}{\nu} \frac{KT}{h\nu_i} \right) \right] \right.$$

$$\left. + 2n_g Q(\nu_i) \nu_i^2 f(\nu) \, Ei(-\xi) \exp\left[-\frac{h\nu_i}{KT} \left(\frac{\nu}{\nu_i} \right) \right] \right\} d\nu = 0 \tag{33}$$

---

*This analysis is valid for any impurity whose absorption cross-section has this frequency dependence. When Argon is the driven gas and Molecular Hydrogen the impurity, corrections to this analysis must be made. These corrections do not radically change the calculated profiles. This will be fully discussed in Ref. 18, where a comparison between theory and experiment is made.

where $\lambda_i = [\, n_g\, Q(\nu_i)]^{-1}$,

$f(\nu)\ \dfrac{Q_i(\nu)}{Q(\nu)}$,

and $\xi = n_g\, Q(\nu)\, x.$

The saddle point of integration in Eq. (33) is at

$$\frac{d}{d\nu}\left[\frac{\nu}{\nu_i} + \frac{x}{\lambda_i}\,\frac{\nu_i}{\nu}\,\frac{KT}{h\nu_i}\right] = 0 \tag{34}$$

or

$$\frac{\nu}{\nu_i} = \sqrt{\frac{x}{\lambda_i}\,\frac{KT}{h\nu_i}} \tag{35}$$

Furthermore, we will let $T = 11,000^{\circ}K$ (the temperature behind the shock), so that

$$\frac{h\nu_i}{kT} = 16.3$$

Also since $x/\lambda_i < 1$, ν/ν_i is less than 1 and the saddle point is located outside the range of integration. Thus Eq. (33) can be expanded asymptotically by using the formula[19]:

$$\int_{s_a}^{\infty} G(s)\, e^{\Omega\tau(s)}\, ds = -\frac{1}{\Omega}\,\frac{G(s_a)\, e^{\Omega\tau(s_a)}}{\tau'(s_a)} - \frac{1}{\Omega}\int_{s_a}^{\infty} \frac{d}{ds}\left[\frac{G(s)}{\tau'(s)}\right] e^{\Omega\tau(s)}\, ds \tag{36}$$

where Ω is a numerical parameter which determines the accuracy of the convergence of the expansion. In our case, $\Omega = h\nu_i/KT = 16.3$. After applying formula (36) consecutively two times, and after considerable

simplification, we get

$$\frac{1.06}{\eta} - 0.058 \cdot 2\, e^{\eta}\, Ei(-\eta) + 0\left(\frac{1}{16.33}\right) = 0 \qquad (37)$$

where $\eta = n_g\, Q(\nu_i)x$.

Equation (37) has been solved graphically and its solution is $\eta_{max.} \simeq 0.6$. The absorption cross-section for H_2 at the ionization edge is

$$Q(\nu_i) \simeq 10^{-17}\ cm^2 \qquad (38)$$

Using the above values, the partial pressure of H_2 at which the peak occurs is obtained as a function of distance ahead of the shock and is plotted in Fig. 2.

IV. B. The Precursor Profile

If a black body source (Eq. 10) is assumed, integration of Eq. (20) (repeated use of Eq. (36) is made) gives the following expression for the precursor profile:

$$n(x) = \frac{A\nu_i^3\, n_g\, Q(\nu_i)}{2U c^2 x}\, e^{-16.3-\eta} \left\{ \frac{1}{16.3}\left[1 + e^{\eta}\, Ei(-\eta)\right] + \left(\frac{1}{16.3}\right)^2 \right\} \qquad (39)$$

This expression is plotted in Fig. 3 for different H_2 pressures (different values of n_g). The increase and eventual decrease with increasing H_2 pressure is clearly seen in the figure.

For a fixed x in Fig. 3, the precursor electron number density as a function of H_2 partial pressure can be obtained. This is plotted in Fig. 4

for x = 50 cm. and x = cm. These curves show the "peak behavior" and the partial pressures at which the peaks occur agree with the values in Fig. 2, which were obtained from a more general analysis.

In Fig. 5, a comparison is made between the precursor profile obtained from this modified theory (at a H_2 partial pressure of 50μ Hg.) and the original Wetzel theory[3] (assuming a one-step photoionization of H_2). The electron number densities obtained from the original Wetzel theory are several orders of magnitude higher and the fall-off with distance ahead of the shock much less rapid than obtained from the modified theory. The experiments in Ref. 18 agree quite well with the modified theory but not at all with the original Wetzel theory.

If $\ell n\ n(x)$ is obtained from Eq. 39, and if this expression is then differentiated, the following equation for the slope of the logarithm of the precursor profile results:

$$-\frac{d}{dx}\,\ell n\, n(x) = \frac{1}{x}\left\{\frac{1+\frac{1+\eta}{16.3}}{\left[1+e^{\eta}\,\eta\ Ei(-\eta)\right]+\frac{1}{16.3}}\right\} \tag{40}$$

Fig. 6 is a plot of this expression as a function of the H_2 partial pressure for a fixed distance, x = 100 cm, ahead of the shock. This curve will be compared with experiment in Ref. 18.

SECTION V

CONCLUDING REMARKS

Until recently, very little experimental data on electron precursors was available. The recent shock tube experiments in Argon[10, 13] provided data on which to test the several theories which have been introduced over the past few years. For one thing, the experiments of Lederman and Wilson strongly suggest that "diffusion theories", at least for the their experiments, do not apply. They showed, experimentally, that radiation from the hot gas behind the shock front was responsible for the observed ionization ahead of the shock. They also found an electron density distribution ahead of the shock which did not change with time in a shock fixed coordinate system. (Holmes[13] did not find this "steady state" situation in his experiments.)

These experiments strongly recommend a photoionization theory like the one proposed by Wetzel[3]. Wetzel's theory postulates a plane source, where in most applications (including the present shock tube application) a point or spherical radiator is more realistic. Moreover, when the precursor number densities due to photoionization of the Argon driven gas is calculated by Wetzel's theory, the levels are found to be several orders of magnitude below the experimental values.

With these limitations of the Wetzel theory in mind, the present modifications of his theory were made:

1) A point or spherical radiator, located at the shock front and moving with the shock velocity, was assumed.

2) The ionization ahead of the shock was viewed not as a one-step photoionization of Argon but as a one-step photoionization of impurities present in the Argon driven gas.

3) Since the radiation, for frequencies below the first ionization edge

of Argon, was not necessarily expected to behave like black body radiation, this question was investigated. It was found that, because of the impurities in the driven gas, a black body radiator is a reasonable one to assume.

As an application of the theory, precursor profiles were calculated for a one-step photoionization of an H_2 impurity (the partial pressure of H_2 was varied from 2 to 75 μHg.). The driven gas was assumed to be Argon at a pressure of 2 mm. Hg.; and the Mach number was assumed to be 13.2, giving a temperature of approximately 11,000°K behind the shock. A comparison is made with the original Wetzel theory, applied to a one-step photoionization of H_2. The electron number densities obtained from the Wetzel theory are several orders of magnitude higher and the fall-off with distance ahead of the shock much less rapid than obtained from the modified theory (Fig. 5). Also, according to the Wetzel theory, the precursor electron number density would decrease with an increase in H_2 partial pressure, whereas the modified theory predicts an increase and eventual decrease with increasing H_2 partial pressure. Experiments have been performed where minute quantities of H_2 were added to the Argon driven gas and changes in the precursor profile were recorded [18]. In all respects, the experiments agree quite well with the modified theory but not at all with the original Wetzel theory.

SECTION VI

REFERENCES

1. Lin, S.C.: Radio Echoes from a Manned Satellite During Reentry. J. Geophys. Res. 67, 3851-3870 (1962).
2. Cook, A., Hawkins, G.S.: The Meteoric Head Echo. Smithsonian Contrib. Astrophys., 5, 1, 1960.
3. Wetzel, L.: Far-Flow Approximations for Precursor Ionization Profiles. AIAA J., 2, 1208-1214 (1964).
4. Clarke, J., Ferrari, C.: Gas Dynamics With Nonequilibrium Radiative and Collisional Ionization. Phys. Fluids, 8, 2121-2139.
5. Murty, S.S.R.: Effect of the Line Radiation on Precursor Ionization. AIAA Radiation Conference, Philadelphia, (1965).
6. Weymann, H.: Electron Diffusion Ahead of Shock Waves in Argon. Phys. Fluids, 4, 545-548, (1960).
7. Petschek, H., Byron, S.: Approach to Equilibrium Ionization Behind Strong Shock Waves in Argon. Annals of Phys. 1, 270-315 (1957)
8. Hollyer, R.. Preliminary Studies in the APL High Temperature Shock Tube. Johns Hopkins University, Applied Physics Lab., Rept. CM-903 (May 1957).
9. Gloersen, P.: Some Unexpected results of Shock-Heating Xenon. Phys. Fluids, 3, 857-870 (1960).
10. Lederman, S., Wilson D.: Microwave Resonant Cavity Measurement of Shock Produced Electron Precursors. AIAA J., 5, 1, 70, (1967).
11. Hammerling, P.: Ionization Effects of Precursor Radiation From Shocks in Air. Avco-Everett Research Lab. Rept. 98 (June 1960).

12. Sturtevant, B.: Application of a Magnetic Mass Spectrometer to Ionization Studies in Impure Shock-Heated Argon. J. Fluid Mech., 25, 641-656 (1966).

13. Holmes, L. B.: Plasma Density Ahead of Pressure Driven Shock Waves. University of Rochester, TNI (May 1965).

14. Jahnke-Emde-Losch,: Tables of Higher Functions. McGraw-Hill, pp. 2 (1960).

15. Abramowitz, M., Stegun, I.: Handbook of Math Functions. N. B. S., June 1964.

16. Niblett, B., Blackman, V. H.: An Approximate Measurement of the Ionization Time Behind Shock Waves in Air. J. Fluid Mech. 4, 191-194 (1958).

17. Cairns, R. B., Samson, J.: Total Absorption Cross Section of Atomic Oxygen Below 910Å. Phys. Review, 139 (5A), 1403-1407 (1965).

18. Wilson, D. S., Lederman, S.: Precursor Ionization Due to Photoionization of H_2 Impurities in Argon Shocks. Polytechnic Institute of Brooklyn, PIBAL Report No. 1033, (to be published).

19. Felsen, L.: Model Analysis and Synthesis of EMT Fields. Chap. IV, PIB. R-776-59.

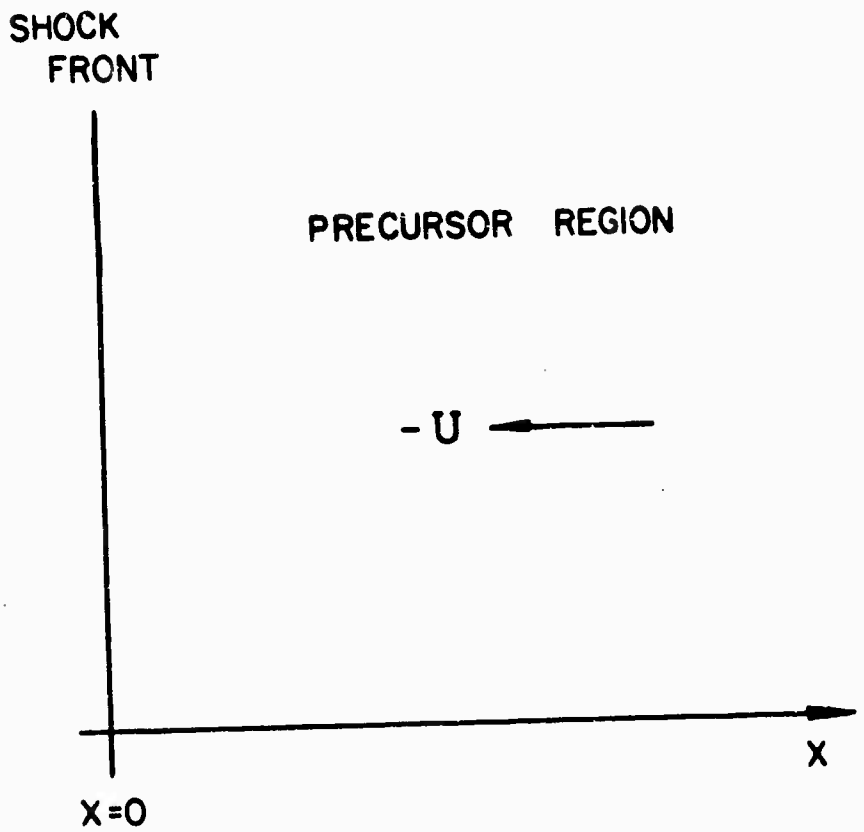

FIG. 1 SHOCK - BASED COORDINATE SYSTEM

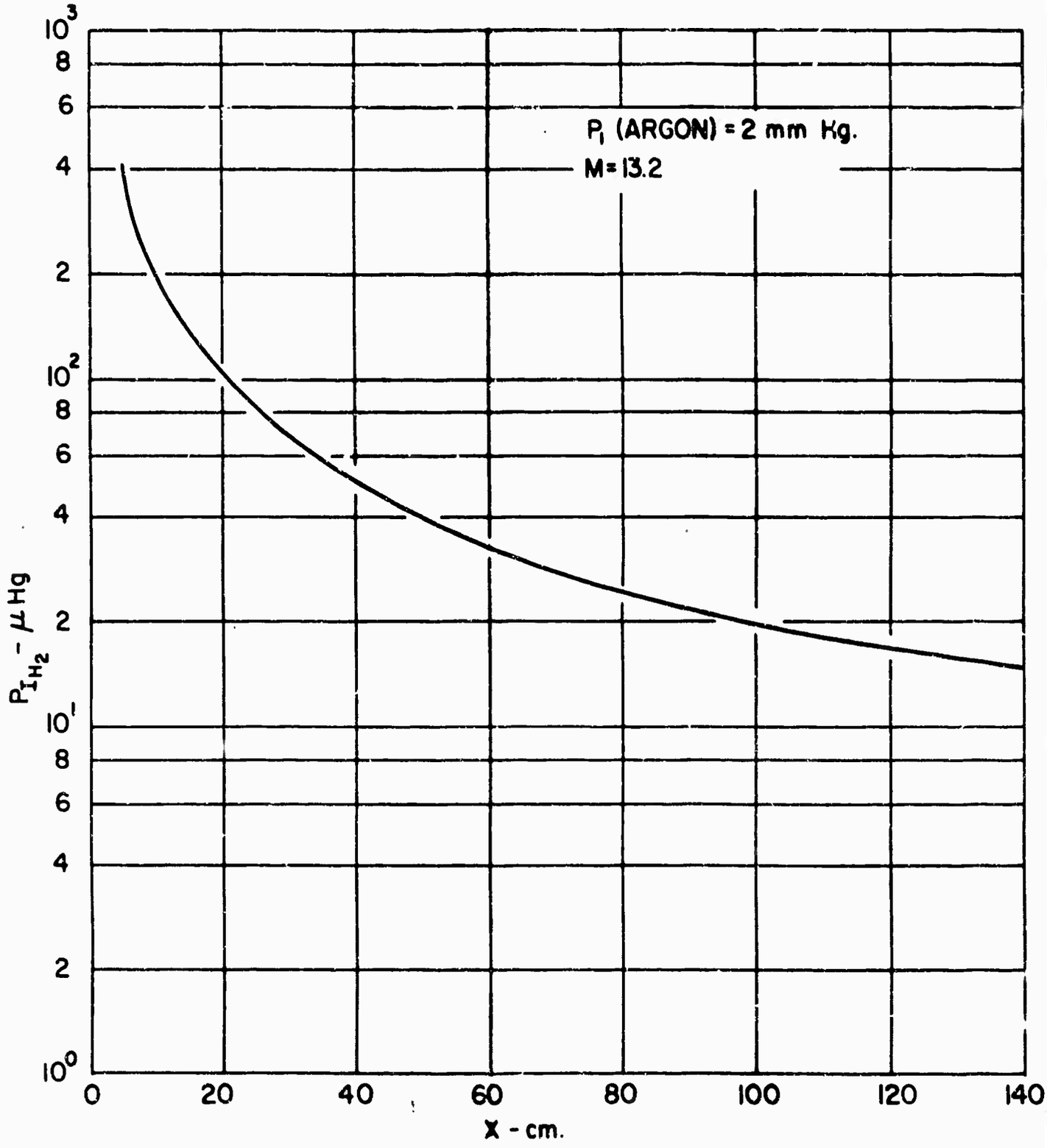

FIG. 2 PARTIAL PRESSURE OF H_2 FOR PEAK PRECURSOR DENSITY VS DISTANCE IN FRONT OF SHOCK

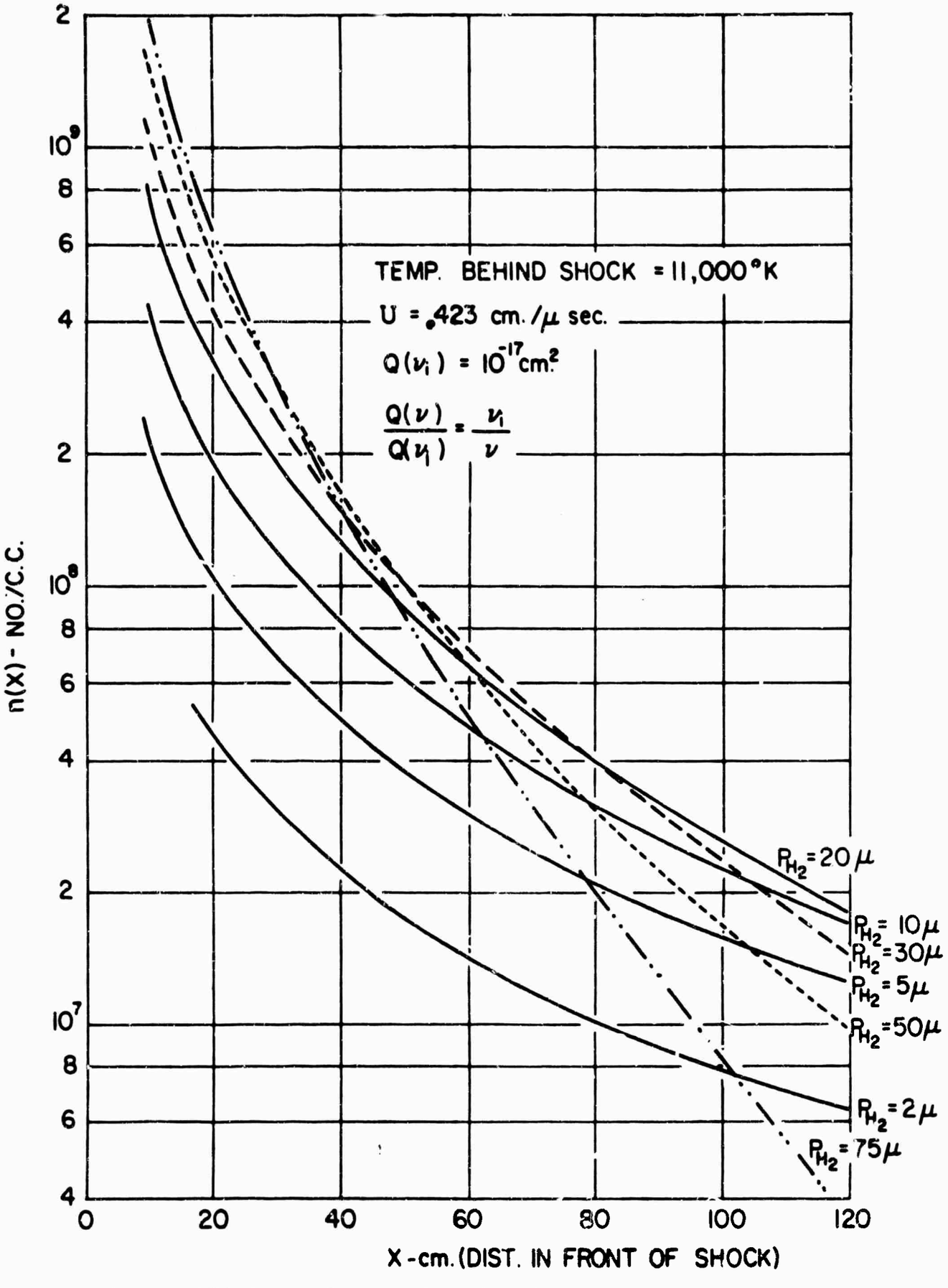

FIG. 3 DEPENDENCE OF PRECURSOR PROFILE ON H_2 PARTIAL PRESSURE

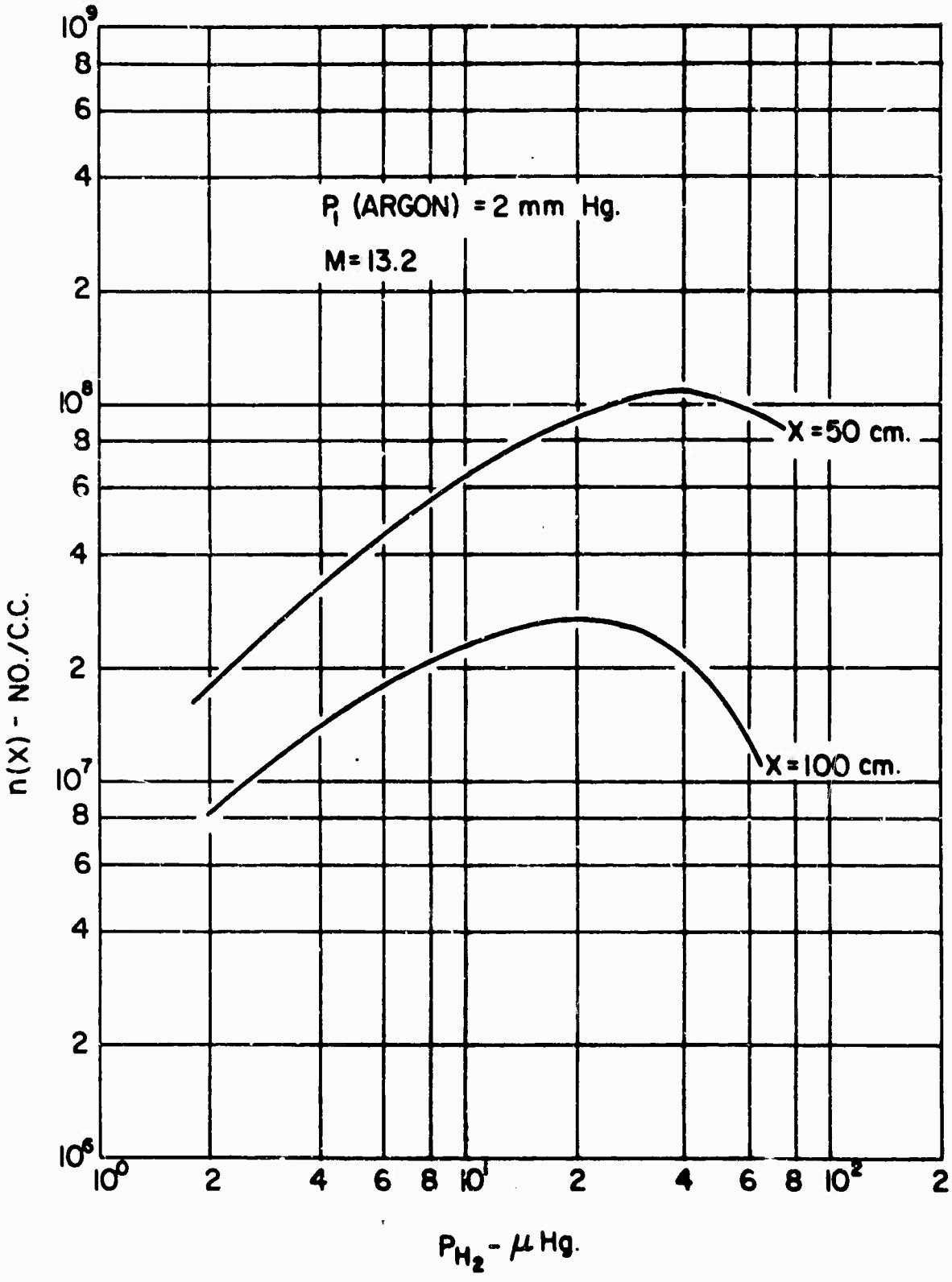

FIG. 4 PRECURSOR NUMBER DENSITY VS H_2 PARTIAL PRESSURE

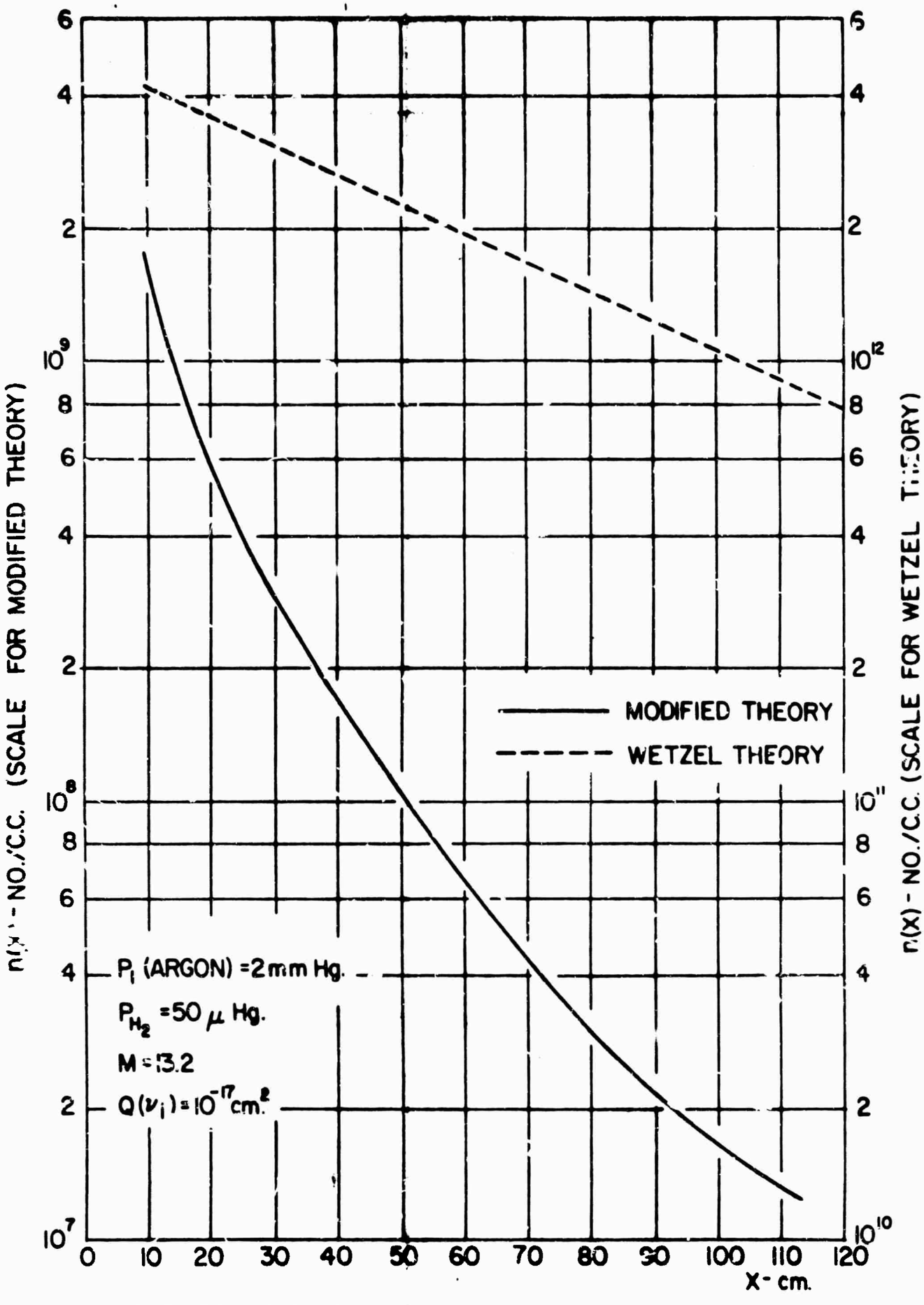

FIG. 5 PRECURSOR NUMBER DENSITY VS DISTANCE IN FRONT OF SHOCK

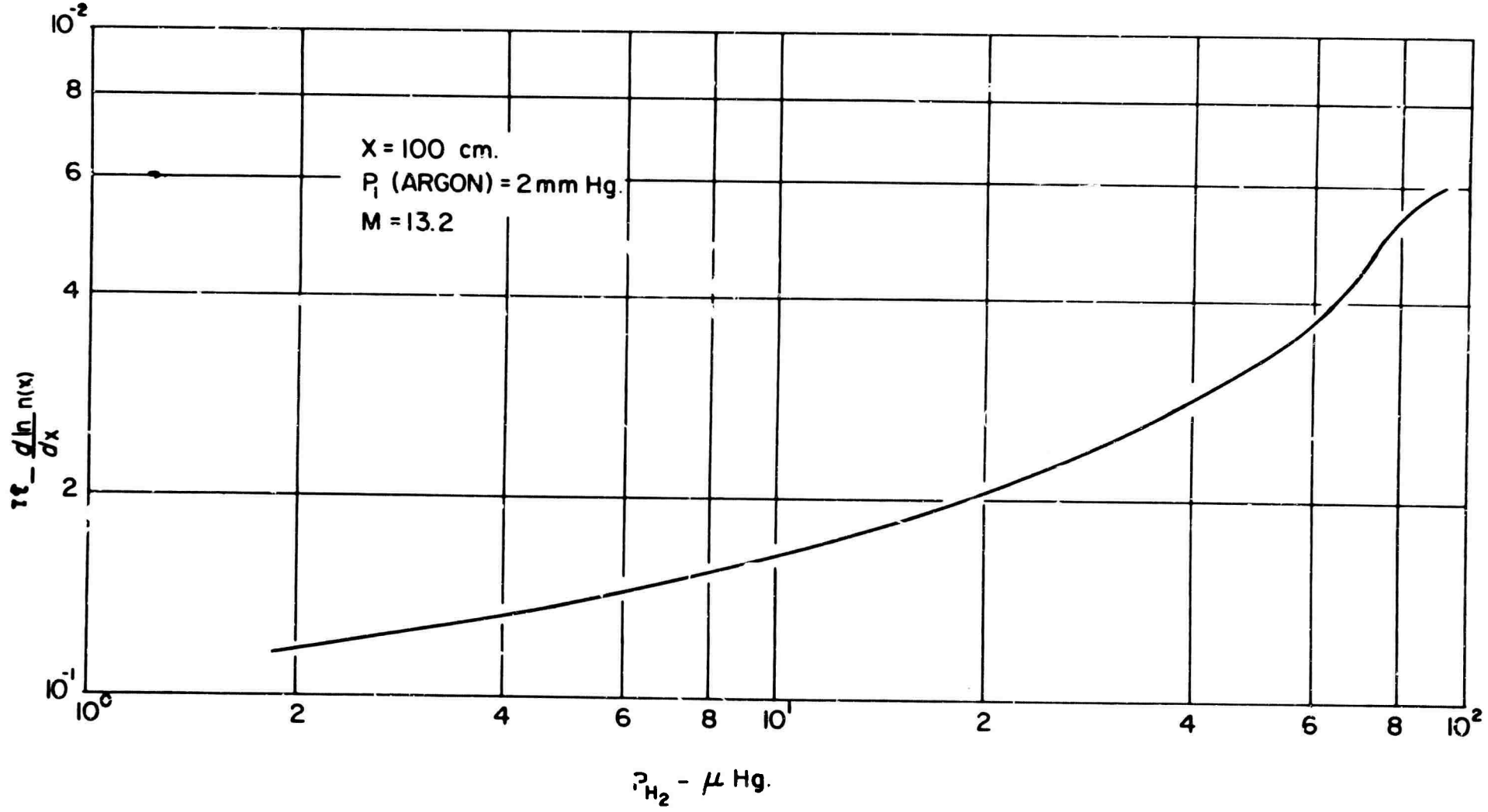

FIG. 6 SLOPES OF PRECURSOR PROFILES VS H_2 PARTIAL PRESSURE

BLANK PAGE

Unclassified

Security Classification

DOCUMENT CONTROL DATA - R & D

(Security classification of title, body of abstract and indexing annotation must be entered when the overall report is classifi

1 ORIGINATING ACTIVITY (Corporate author)

Polytechnic Institute of Brooklyn
Dept. of Aerospace Engrg. and Applied Mechanics
Route 110, Farmingdale, New York 11735

2a. REPORT SECURITY CLASSIFICATION: Unclassified

2b. GROUP

3 REPORT TITLE

IMPURITY PHOTOIONIZATION THEORY OF PRECURSORS

4 DESCRIPTIVE NOTES (Type of report and inclusive dates)

Research Report

5 AUTHOR(S) (First name, middle initial, last name)

Daniel S. Wilson and Tony C. Lin

6 REPORT DATE: October 1967

7a. TOTAL NO. OF PAGES: 31

7b. NO. OF REFS: 19

8a. CONTRACT OR GRANT NO: Nonr 839(38)

b. PROJECT NO.

c. ARPA Order No. 529

d.

9a. ORIGINATOR'S REPORT NUMBER(S): PIBAL REPORT No. 1006

9b. OTHER REPORT NO(S) (Any other numbers that may be assigned this report)

10. DISTRIBUTION STATEMENT

Distribution of this document is unlimited.

11. SUPPLEMENTARY NOTES

12. SPONSORING MILITARY ACTIVITY

Office of Naval Research
Department of the Navy
Washington, D. C.

13 ABSTRACT

An extension of Wetzel's theory is proposed to explain electron precursor phenomena in pressure driven shock tubes. The theory is based on the assumption which has been experimentally verified, that radiation from the hot gas behind the shock front is responsible for the precursor effect. A point radiator, located at the shock front and moving with the shock velocity, is assumed. It is shown that this radiator can be idealized by a black body. The precursor electron density is derived from a one-step photoionization of the impurities present in the driven gas.

As an application of the theory, precursor profiles are calculated for an H_2 is varied from 2 to 75μ Hg. The temperature behind the shock is assumed to be 11,000°K

DD FORM 1 NOV 68 1473

Unclassified

Security Classification

14. KEY WORDS	LINK A		LINK B		LINK C	
	ROLE	WT	ROLE	WT	ROLE	WT
Precursor Ionization						
Electron Density						
Shock Tubes						